INSTITUT FÜR INFORMATIK

# A Fast and Robust Optimization Methodology for a Marine Ecosystem Model Using Surrogates

M. Prieß, S. Koziel, T. Slawig

Bericht Nr. 1110
November 8, 2011
ISSN 2192-6247


CHRISTIAN-ALBRECHTS-UNIVERSITÄT

ZU KIEL

Institut für Informatik der
Christian-Albrechts-Universität zu Kiel
Olshausenstr. 40
D – 24098 Kiel

# A Fast and Robust Optimization Methodology for a Marine Ecosystem Model Using Surrogates

M. Prieß, S. Koziel, T. Slawig

Bericht Nr. 1110
November 8, 2011
ISSN 2192-6247

e-mail: mpr@informatik.uni-kiel.de, koziel@ru.is,
ts@informatik.uni-kiel.de

# A Fast and Robust Optimization Methodology for a Marine Ecosystem Model Using Surrogates

M. Prieß[a,1,*], S. Koziel[c], T. Slawig[a]

[a] *Institute for Computer Science, Cluster The Future Ocean, Christian-Albrechts Universität zu Kiel, 24098 Kiel, Germany*
[b] *Leibniz Institute of Marine Science (IFM-GEOMAR), Marine Biogeochemistry, Biological Oceanography, Düsternbrooker Weg 20, 24105 Kiel, Germany*
[c] *Engineering Optimization & Modeling Center, School of Science and Engineering, Reykjavik University, Menntavegur 1, 101 Reykjavik, Iceland*

**Abstract**

Model calibration in climate science plays a key role for simulations and predictions of the earth's climate system. Straightforward attempts by employing the high-fidelity (or fine) model under consideration directly in an optimization loop using conventional optimization algorithms are often tedious or even infeasible, since typically a large number of computationally expensive fine model evaluations are required. The development of faster methods becomes critical, where the optimization of coupled marine ecosystem models, which simulate biogeochemical processes in the ocean, are a representative example. In this paper, we introduce a surrogate-based optimization (SBO) methodology where the expensive fine model is replaced by its fast and yet reasonably accurate surrogate. As a case study, we consider a representative of the class of one-dimensional marine ecosystem models. The surrogate is obtained from a temporarily coarser discretized physics-based low-fidelity (or coarse) model. and a multiplicative response correction technique. In our previous work, a basic formulation of this surrogate was sufficient to create a reliable approximation, yielding a remarkably accurate solution at low computational costs. This was verified by model generated, attainable data. The application on real data is covered in this paper. Enhancements of the basic formulation by utilizing additionally fine and coarse model sensitivity information as well as

*Corresponding author (*phone:* +49-(0)431 880 7452, *fax:* +49-(0)431 880 7618)
*Email addresses:* mpr@informatik.uni-kiel.de (M. Prieß), koziel@ru.is (S. Koziel), ts@informatik.uni-kiel.de (T. Slawig)

[1] Research supported by DFG Cluster The Future Ocean

trust-region convergence safeguards allow us to further improve the robustness of the algorithm and the accuracy of the solution. The trade-offs between the solution accuracy and the extra computational overhead related to sensitivity calculation will be addressed. We demonstrate that SBO is able to yield a very accurate solution at still low computational costs. The optimization process – when compared to the direct fine model optimization – is significantly speed up to about 85%.
*Keywords:* Climate models, marine ecosystem models, surrogate-based optimization, parameter optimization, response correction, efficient optimization, surrogate

## 1. Introduction

Numerical simulations play a key role to simulate and predict processes in the earth's climate system, ranging from fluid mechanics, as in the atmosphere and ocean, to bio- and biochemical interactions, e.g., in marine or other type of ecosystems. The underlying models are typically given as time-dependent partial differential or differential algebraic equations (PDEs/DAEs) [10, 17, 19].

Since many important processes are non-linear, the numerical effort to simulate the whole or parts of the climate system with a satisfying accuracy and resolution is quite high. This motivates the development and use of reduced order models by e.g. coarser discretizations (in time and/or space) or by parametrizations to reduce the system size and thus the computational effort [19]. Through those parametrizations, several additional parameters enter the system. Many of them are not known beforehand and not directly measurable. Before a transient simulation of a model (e.g., used for predictions) is possible, the latter has to be calibrated and validated w.r.t. measurement data, i.e., relevant unknown parameters have to be identified using large-scale optimization methods. Growth and dying rates in marine ecosystem models [7, 26], one of which is taken as a test case for the proposed optimization methodology, are examples for such unknown parameters. Marine ecosystem models describe photosynthesis and other biogeochemical processes in the marine ecosystem that are important, e.g., to compute and predict the oceanic uptake of carbon dioxide ($CO_2$) as part of the global carbon cycle [26].

The mathematical task of parameter optimization can be classified as a least-squares

type optimization or inverse problem [2, 3, 31]. This optimization (or calibration) process requires a substantial number of (typically expensive) function and optionally sensitivity or even Hessian matrix evaluations.

Straightforward attempts by employing the *high-fidelity* or *fine* model under consideration directly in an optimization loop using conventional optimization algorithms are therefore tedious or even infeasible, especially when using traditional, gradient-based techniques. The need for an accelerated optimization process, which especially becomes important while handling complex three-dimensional models, becomes critical.

Surrogate-based optimization (SBO) addresses this issue by shifting the computational burden from the accurate and expensive high-fidelity model to its fast but yet reasonably accurate surrogate. More specifically, the idea of SBO is to replace the fine model in the optimization process in the sense of providing predictions of the model optimum. The surrogate can be created by approximating sampled fine model data (so-called *function-approximation surrogates*, see [23, 28, 29]) or by employing a physics-based *low-fidelity* or *coarse* model, a computationally cheap representation of the fine model. The latter approach is used in this paper. Since the accuracy of the coarse model is usually not sufficient to directly use the latter in an optimization loop, it is often necessary to use suitable alignment/correction techniques to reduce the misalignment between the coarse and fine model responses. Popular correction/alignment techniques include response correction [30] and space mapping [1]. Surrogate-based optimization is widely and very successfully used in engineering sciences, compare for example [1, 9, 15, 23].

As a case study, in order to investigate the applicability of a SBO methodology to the optimization of marine ecosystem models, we consider a representative of the class of one-dimensional models. Clearly, the computational effort in a one-dimensional simulation is significantly smaller than in the three-dimensional case. However, since biochemistry mainly happens locally in space and since the complexity of the biogeochemical processes included in this specific model is high, this model serves as a good test example for the applicability of SBO approaches, before considering computationally more expensive three-dimensional models.

One straightforward way to introduce a physics-based coarse model is to reduce the spatial

and/or temporal resolution, whereas the latter is used for the selected model in this paper. We use a multiplicative response correction technique for the alignment of the coarse and fine model response.

In our previous work [22], a basic formulation of this surrogate was sufficient to create a reliable approximation, yielding a remarkably accurate solution at low computational costs. This was verified by model generated, attainable data.

In this paper, the application on real data is covered. Utilizing additionally fine and coarse model sensitivity information ensures the zero- and first-order consistency conditions between the fine model and the surrogate, i.e., agreement in function values and first-order derivatives. In conjunction with trust-region convergence safeguards [4, 13], this allows us to further improve the robustness of the SBO and accuracy of its solution. The trade-offs between the solution accuracy and the extra computational overhead related to sensitivity calculation will be addressed.

We show the results of an exemplary SBO run and compare the solution to those obtained by a direct fine and coarse model optimization. We demonstrate that a direct optimization of the fine model requires a substantial number of comparably expensive fine model evaluations whereas a direct coarse model optimization is computationally cheap but yields a rather inaccurate solution only. We finally show that SBO yields a solution close to the one obtained by a direct fine model optimization while greatly reducing the optimization costs – down to 15% of those of a direct fine model optimization.

The structure of the paper is as follows: We briefly describe the general form of numerical model used in climate science and highlight the special properties of marine ecosystem models in Section 2 (see also [22]). We introduce the basic idea of surrogate-based optimization in Section 3. The ecosystem model and corresponding optimization problem, which is taken as an example in this paper, is introduced in Section 4. The coarse model that we use as a basis to create a surrogate, is recalled in Section 5 (see again [22]). The response correction approch used to obtain the surrogate is motivated and described in Section 6. The optimization setup, numerical results and discussion of exemplary test runs are provided in Sections 7 and 8. Section 9 concludes the paper with a summary and an outlook.

## 2. Climate Models – A General Formulation

Numerical models that are used to simulate processes in the climate system (what we denote by *climate models*) can be quite generally written as coupled systems of time-dependent partial differential or differential algebraic equations (PDEs/DAEs) [10, 17, 19], for example in the following form:

$$\begin{aligned} E\,\frac{\partial y}{\partial t} &= f(y,u) \quad && \text{in } I\times\Omega \\ y(t_0,\mathbf{x}) &= y_{init} && \text{in } \Omega \\ By &= 0 && \text{on } I\times\Gamma, \end{aligned} \tag{1}$$

where $y(t,x) : I \times \Omega \to \mathbb{R}$ is the vector of the *state variable*, with a definite time interval $I = [t_0, t_0 + T]$, $t_0 \in \mathbb{R}$ an initial point in time, $T \in \mathbb{R}$ a duration, $\Omega \in \mathbb{R}^3$ a domain and where $\Gamma = \partial\Omega$ denotes its boundary. The time variable is denoted by $t \in I$ and the spacial variable by $\mathbf{x} = (x_1, x_2, x_3)^\top \in \overline{\Omega}$. We used a boldfaced notation to distinguish a vector from a continous or scalar variable in the following.

The right-hand side $f$ includes all spatial differential operators as well as the coupling between the components of the state variable $y$. In climate models, it often additionally depends explicitly on the space and time variables $x$ and $t$, respectively, which, for simplicity, is omiited in the notation. Moreover, $f$ depends on a number of model parameters which are summarized in the vector $u$. The vector-valued function $y_{init} : \Omega \to \mathbb{R}$ includes the initial model data and $B$ denotes the boundary operator which – when representing for example a Neumann boundary condition – is nonlinear and includes the first normal derivative.

$E$ is a matrix with the size of $y$, typically being the identity matrix for a PDE while having rank deficiency for a PDAE [14]. We include PDAEs in this formulation since for example in ocean circulation models [10], the underlying Navier-Stokes equations are – when written in the above form – a PDAE system. Then $y$ may for example consist of the velocity, pressure, temperature or salinity field. In the case of marine ecosystem models, which are formulated as a PDE system, the matrix $E$ can be set to the identity and thus omitted. In this case, the state vector $y$ contains so-called *biogeochemical tracers* such as phyto- and zooplankton,

see Section 2.1 below and 4 for details.

### *2.1. Marine Ecosystem Models*

Marine ecosystem models mainly consist of two parts, namely the ocean circulation and the biogeochemical model. The coupling between ocean circulation and the biogeochemical interactions such as photosynthesis is mostly regarded as a one-way coupling. This means that the influence of the biota on the circulation (including temperature and maybe salinity distribution) is assumed to be negligible and thus is often omitted (so-called *off-line* mode). Velocity and temperature fields are computed beforehand by an ocean circulation model and only used as *forcing data* for the biogeochemical simulations which significantly reduces the compuational effort. Our example model (cf. Section 4) uses this off-line mode.

The model equations consist of a system of coupled advection-diffusion-reaction equations, where the reaction terms (also called *source minus sink*, or *sms* terms) are given by the biogeochemical interactions between the biogeochemical tracers. As a special form of (1), a system of these *transport equations* for $n_t$ tracers then generally reads

$$\frac{\partial y_i}{\partial t} = \operatorname{div}(\kappa \nabla y_i) - \operatorname{div}(v y_i) + q_i(y, \mathbf{u}), \quad i = 1, \ldots, n_t \tag{2}$$

where $y_i(t, x) : I \times \Omega \to \mathbb{R}$ denotes the concentration of tracer $i$ at time $t$ and the spatial location $x$. If no interactions with the atmosphere is taken into account, homogeneous Neumann conditions on the boundary $\Gamma$ for all concentrations are employed, i.e.,

$$\frac{\partial y_i}{\partial n} = n \cdot \nabla y = 0 \quad \text{on } I \times \Gamma, \quad i = 1, \ldots, n_t, \tag{3}$$

where $n$ denotes the normal vector. The time dependent turbulent mixing/diffusion coefficient $\kappa(t, x) : I \times \Omega \to \mathbb{R}$ as well as the velocity vector field $v(t, x) : I \times \Omega \to \mathbb{R}^3$ with $v = (v_i)_{i=1,2,3}$, both satisfy the Navier-Stokes equations. Since the parameters $\mathbf{u} \in \mathbb{R}^{n_p}$, which are subject to the parameter optimization, are scalar coefficients in the nonlinear biogeochemical coupling terms $q_i$, we use a boldfaced notation.

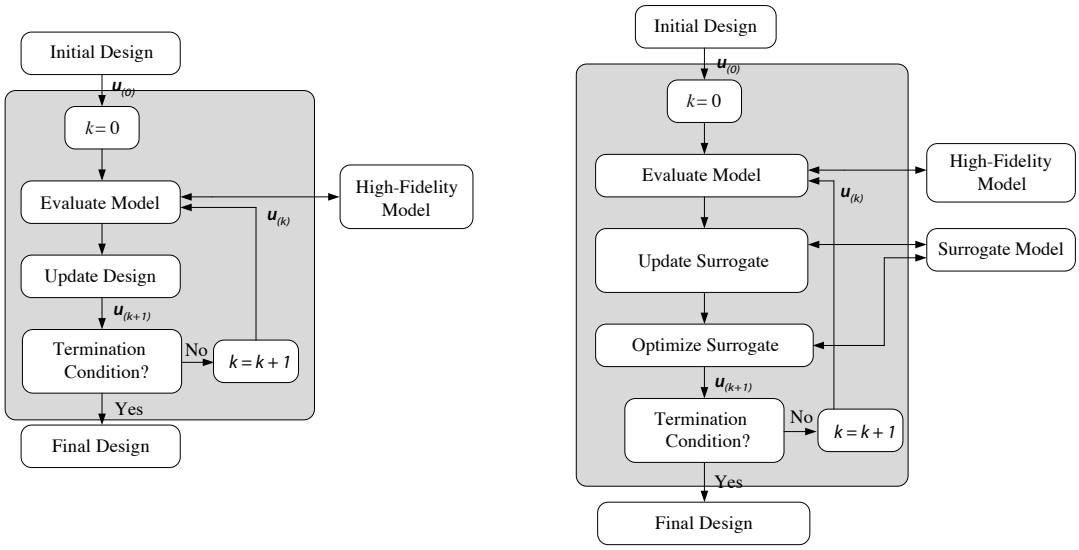


(a) Direct Optimization. (b) Surrogate-Based Optimization.

Figure 1: In a direct optimization (Figure 1a), the complex high-fidelity or fine model under consideration is directly used in an optimization loop using conventional (deterministic/local or stochastic/global) optimization approaches. In a surrogate-based approach (Figure 1b), the fine model is replaced in the optimization loop in iteration $k$ by its computationally cheaper but yet reasonably accurate surrogate. Here, $\mathbf{u}_k$ denotes the parameter vector at iteration $k$.

## 3. Surrogate-Based Optimization

For many optimization problems, a high computational cost or even the lack of sensitivity information of the model under consideration is a major bottleneck.

The optimization problem typically is to solve for a solution of a minimization problem, which can quite generally be formulated as

$$\min_{\mathbf{u}} J(\mathbf{y}(\mathbf{u})) \tag{4}$$

where $J$ denotes a cost function measuring the misfit between relevant quantities (which are obtained from the discrete model response $\mathbf{y}$ at the parameters/design $\mathbf{u}$) and some desired specifications. For the considered optimization problem in this paper for example, these quantities are tracer concentrations, whereas the desired specifications are given measurement data. Also, for some applications, the optimization problem could include both, a minimization and a maximization. However, for the purpose of this section, to sketch the

basic ideas of SBO, we omit such a formulation as well as any detailed description of $J$ here.

Straightforward attempts by employing the high-fidelity (or fine) model under consideration directly in an optimization loop (cf. Figure 1a) using conventional optimization algorithms are often tedious or even infeasible, since typically a large number of the expensive fine model evaluations are required. The need for an accelerated optimization process becomes critical, for which the optimization of complex marine ecosystem models is a representative example.

Surrogate-based optimization (SBO) [1, 9, 15, 23] addresses these issues by replacing the original fine model in the optimization loop by its computationally cheaper but yet reasonably accurate surrogate (cf. Figure 1b). In particular, the surrogate at the iterate $\mathbf{u}_k$, in the following denoted by $\mathbf{s}_k(\mathbf{u})$, is contructed typically using available fine model data from the current and possibly also from previous iterates $(\mathbf{u}_i)_{i=0,\dots,k-1}$.

Possible ways to create a surrogate are through approximations of sampled fine model data (cf. Section 3.1) or by correction/alignment of a less accurate but computationally cheaper low-fidelity (or coarse) model (cf. Section 3.2).

The next iterate, $\mathbf{u}_{k+1}$, in a SBO scheme is obtained by optimizing the surrogate $\mathbf{s}_k$, i.e.,

$$\mathbf{u}_{k+1} = \operatorname*{argmin}_{\mathbf{u}} J\,(\,\mathbf{s}_k(\mathbf{u})\,). \tag{5}$$

assuming some general cost functional $J$ as in (4). The process of updating the surrogate and subsequent optimization is repeated a user-defined termination condition is satisfied, which can use certain convergence criteria, assumed level of cost function value or a specific number of iterations (particularly if the computational budget of the optimization process is limited).

A well performing surrogate-based algorithm is capable of yielding a reasonably accurate solution at a low computational cost, typically corresponding to only a few evaluations of the fine model. Key prerequisites to ensure this, are a cheap and yet reasonably accurate coarse model as well as a properly selected and low-cost alignment procedure (i.e., using a limited number of fine model evaluations, preferably just one).

### *3.1. Functional Surrogates*

One possibility, which will not be addressed further in this paper, is to create the surrogate by approximating sampled fine model data using suitable techniques, e.g., polynomial regression [23], kriging [28] or support-vector regression [29]. Since these so-called *function-approximation surrogates* are constructed without any particular knowledge of the system they are easily transferable to other application areas. On the other hand, these surrogates do not inherit any physical information about the fine model under consideration and normally require substantial amount of fine model data samples to ensure good accuracy.

### *3.2. Physics-Based Surrogates*

Another possibility, explored in this paper, is to construct the surrogate from a physics-based *low-fidelity* or *coarse* model, a usually computationally much cheaper but – on the other hand – less accurate representation of the fine one. Since the accuracy of the coarse model is typically not sufficient to directly directly replace the fine model in an optimization loop, it is then necessary to use suitable alignment/correction techniques to reduce the misalignment between the coarse and fine model responses and to ensure that the corrected model (the surrogate) provides a reliable prediction of the fine model optimum.

There are several methods of constructing the surrogate from a physics-based low-fidelity model. They include, among others, space mapping (SM) [1], various response correction techniques [30], manifold mapping [5], and shape-preserving response prediction (SPRP) [12]. An appropriate response correction technique is usually rather problem-specific.

These so-called *physics-based surrogates*, when the underlying coarse model and alignment technique is chosen properly, inherit relevant physical characteristics of the original fine model so that only a few fine model data is necessary to ensure a sufficient accuracy. Also, generalization capability of the physics-based models is typically much better than for functional ones. As a results, SBO schemes working with physics-based surrogates normally require small number of fine model evaluations to yield a satisfactory solution. On the other hand, their transfer to other applications is less straightforward since the underlying coarse model and chosen correction approach is rather problem specific..

Possible ways to create the underlying physical coarse model are by using a coarser discretization in time and/or space (while employing the same simulation tool as for the fine

model), simplified physics or different ways of describing the same physical phenomenon or even by using analytical formulas if available.

The surrogate, we use in this paper is physics-based. The specific coarse model is obtained by a coarser time discretization (cf. Section 5) which is further aligned by using a multiplicative response correction (cf. Section 6).

### *3.3. Consistency Conditions and Convergence of SBO*

Provided that the surrogate $\mathbf{s}_k$ satisifes so-called zero- and first-order consistency conditions with the original fine model $\mathbf{y}_f(\mathbf{u}_k)$ at the iterate $\mathbf{u}_k$, i.e., agreement between the function values and first-order derivatives at the current iteration point, mathematically written as

$$\mathbf{s}_k(\mathbf{u}_k) = \mathbf{y}(\mathbf{u}_k), \quad \mathbf{s}_k'(\mathbf{u}_k) = \mathbf{y}'(\mathbf{u}_k), \tag{6}$$

the surrogate-based scheme (5) is provable convergent to at least a local optimum of (4) under mild conditions regarding the coarse and fine model smoothness, and provided that the surrogate optimization scheme is enhanced by the trust-region (TR) safeguard, i.e.,

$$\mathbf{u}_{k+1} = \underset{\substack{\mathbf{u}\in U_{ad},\\ \| \mathbf{u}-\mathbf{u}_k \| \leq \delta_k}}{\operatorname{argmin}} \; J\left( \mathbf{s}_k(\mathbf{u}) \right), \tag{7}$$

with $\delta_k$ being the trust-region radius updated according to the TR rules. We refer the reader to e.g. [4, 13] for more details.

In (6), $\mathbf{y}'$ and $\mathbf{s}_k'$ denote the derivatives of the model response w.r.t. the parameter vector $\mathbf{u}$ and at the point $\mathbf{u}_k$, i.e., generally defined as

$$\mathbf{y}'(\mathbf{u}_k) := \left. \frac{\mathrm{d}\,\mathbf{y}}{\mathrm{d}\,\mathbf{u}} \right|_{\mathbf{u}=\mathbf{u}_k}. \tag{8}$$

The surrogate in this paper uses both fine model sensitivity information as well as trust-region convergence safeguards to increase the robustness of the optimization procedure and the accuracy of the solution.

## 4. Example: A Marine Ecosystem Model

The model developed by **(author?)** [20] is a coupled system of four tracers with dissolved inorganic nitrogen ($N$), phytoplankton ($P$), zooplankton ($Z$), and detritus ($D$), thus also called $NPZD$ model, in the following summarized in the tracer or state vector $y = (y_i)_{i=1,\dots,n_t}$ with $n_t = 4$.

The $NPZD$ model simulates the tracer concentrations in one water column at a given horizontal position. This is motivated by the fact that there have been special time series studies at fixed locations [27]. Clearly, the computational effort in a one-dimensional simulation is significantly smaller than in the three-dimensional case. However, since biochemistry mainly happens locally in space and since the complexity of the biogeochemical processes included in this specific model is high, this model serves as a good test example for the applicability of SBO approaches.

The model basically fits into our general framework (2). In the specific $NPZD$ model considered here, no advection term "$\mathrm{div}(vy_i)$" as in (2) is used, since a reduction to vertical advection would make no sense. Starting from a general *continuous* formulation, the model is governed by the equations

$$\frac{\partial y_i}{\partial t} = \partial_z \left(\kappa\, \partial_z y_i\right) + q_i(y, \mathbf{u}), \quad i = 1, \dots, 4, \tag{9}$$

where $z$ denotes the vertical coordinate and where the coupling terms $q_i(y, \mathbf{u})$ are explicitly given as

$$\begin{aligned}
q_1(y,u) &= \Phi_m^z\, y_3 + \gamma_m\, y_4 - J(y_1, y_2, t, z)\, y_2,\\
q_2(y,u) &= J(y_1, y_2, t, z) y_2 - G(y_2, \epsilon, g)\, y_3 - \Phi_m^p\, y_2,\\
q_3(y,u) &= \beta\, G(y_2, \epsilon, g)\, y_3 - \Phi_m^z\, y_3 - \Phi_z^*\, (y_3)^2,\\
q_4(y,u) &= (1-\beta)\, G(y_2, \epsilon, g)\, y_3 + \Phi_m^p\, y_2 + \Phi_z^*\, (y_3)^2\\
&\qquad - \gamma_m\, y_4 - w_s\, \partial_z y_4.
\end{aligned} \tag{10}$$

The system involves an explicit *sinking velocity* $w_s$ for the tracer detritus, and a non-differentiability, namely in the *growth rate of phytoplankton*, which is modeled after the

minimum principle of von Liebig [16] as

$$J(y_1, y_2, t, z) = \min\left\{\bar{\mu}(y_2, t, z), V_p \cdot u(y_1, t, z)\right\}, \tag{11}$$

where the analytical solution for the *light-limited growth rate*, denoted as $\bar{\mu}(y_2, t, z)$, is given according to **(author?)** [6], integrated down to the given depth $z$ [20, 25]. Here, additional parameters $\alpha, k_w$ and $\kappa$ are involved (cf. Table 1).

The *factor for nutrient limited growth of phytoplankton* $u$ and the *maximal phytoplankton growth rate* $V_p$ are given as

$$u(y_1, t, z) = \frac{y_1}{k_N + y_1}, \quad V_p = \mu_m \cdot (C_{ref})^{c\,\Theta(t,z)}, \tag{12}$$

where the parameters $k_N, C_{ref}$ and $c$ are briefly described in Table 1 and where $V_p$ further depends on the water temperature $\Theta$, which has to be provided by an ocean circulation model. Due to the minimum in the growth rate of phytoplankton in (11), the model becomes non-differentiable. Another nonlinear term in the equations is the *zooplankton grazing function* $G$ given as

$$G(y_2, \epsilon, g) = \frac{g\,\epsilon\,(y_2)^2}{g + \epsilon\,(y_2)^2}, \tag{13}$$

which describes the transfer from phytoplankton to zooplankton and detritus with the parameters $\epsilon$ and $g$ again briefly described in Table 1. There are totally twelve model parameters subject to the optimization, which are all summarized in Table 1. For the purpose of this paper to demonstrate the applicability of the proposed SBO approach, we don't want to provide more details on the model and the involved parameters. We refer the reader to [20, 25, 27] for a more thorough description.

### *4.1. Carbon Primary Production*

In addition to the tarcers $N, P, Z$ and $D$, the so-called *carbon fixation* or *carbon primary production* measured as carbon uptake (denotes as $CUP$ in the following) is additionally taken into account in the optimization process for this model [25, 27] (see also below, Section

Table 1: Model parameters (cf. Section 4). Those included in the parameter vector $\mathbf{u} = (\mathbf{u})_{i=1,\ldots,12}$ are subject to the optimization.

| $u_i$ | symbol | value/range | unit (d=86400 s) | parameter meaning |
|---|---|---|---|---|
| | $C_{ref}$ | 1.066 | 1 | growth coefficient |
| | $c$ | 1 | $^\circ\mathrm{C}^{-1}$ | growth coefficient |
| | $R$ | 6.625 | 1 | molar carbon to nitrogen ratio (*redfield ratio*) |
| | $k_w$ | 25 | $\mathrm{m}^{-1}$ | PAR extinction length |
| $u_1$ | $\beta$ | $[0,1]$ | 1 | assimilation efficiency of zooplankton |
| $u_2$ | $\mu_m$ | $\mathbb{R}_0^+$ | $\mathrm{d}^{-1}$ | phytoplankton growth rate parameter |
| $u_3$ | $\alpha$ | $\mathbb{R}_0^+$ | $\mathrm{m}^2\mathrm{W}^{-1}\mathrm{d}^{-1}$ | slope of photosynthesis versus light intensity |
| $u_4$ | $\Phi_m^z$ | $\mathbb{R}_0^+$ | $\mathrm{d}^{-1}$ | zooplankton loss rate |
| $u_5$ | $\kappa$ | $\mathbb{R}_0^+$ | $\mathrm{m}^2(\mathrm{mmol\ N})^{-1}$ | light attenuation by phytoplankton |
| $u_6$ | $\epsilon$ | $\mathbb{R}_0^+$ | $\mathrm{m}^6(\mathrm{mmol\ N})^{-2}\mathrm{d}^{-1}$ | grazing encounter rate |
| $u_7$ | $g$ | $\mathbb{R}_0^+$ | $\mathrm{d}^{-1}$ | maximum grazing rate |
| $u_8$ | $\Phi_m^p$ | $\mathbb{R}_0^+$ | $\mathrm{d}^{-1}$ | phytoplankton linear mortality |
| $u_9$ | $\Phi_z^*$ | $\mathbb{R}_0^+$ | $\mathrm{m}^3(\mathrm{mmol\ N})^{-1}\mathrm{d}^{-1}$ | zooplankton quadratic mortality |
| $u_{10}$ | $\gamma_m$ | $\mathbb{R}_0^+$ | $\mathrm{d}^{-1}$ | detritus remineralization rate |
| $u_{11}$ | $k_N$ | $\mathbb{R}_0^+$ | $\mathrm{mmol\ Nm}^{-3}$ | half saturation for $NO_3$ uptake |
| $u_{12}$ | $w_s$ | $\mathbb{R}_0^+$ | $\mathrm{m\ d}^{-1}$ | detritus sinking velocity |

4.4). For a given depth $z$ and time $t$, it can be briefly formulated as

$$J(y_1, y_2, t, z) \cdot y_2(t, z) \cdot R$$

where $R$ denotes the *Redfiled ratio* [27]. It depends non-linearly on the states $y_1$ and $y_2$, i.e., the tracers dissolved inorganic nitrogen ($N$) and phytoplankton ($P$). It states that the relation between carbon ($C$), nitrogen ($N$) and phosphorus ($P$) in marine phytoplankton is given as $\mathrm{C:N:P} = 106:16:1$. Thus $N$ can be used as a model variable from which the potential uptake of $CO_2$ can be estimated (assuming that there is no limit on phosphorus $P$ and carbon dioxide $CO_2$ in the water). The carbon primary production obeys a daily cycle (cf. Figure 2), since the growth of phytoplankton, $J(y_1, y_2, t, z)$, is light limited due to the term $\bar{\mu}(y_2, t, z)$ (see (11) and [27] for details). The state CUP is calculated internally in the model simuation and provided as an additional part of the model response $y$.

*4.2. Numerical Solution*

In an off-line coupled marine ecosystem model (as for example the $NPZD$ model considered here), there are two ways to make use of the precomputed ocean circulation data. One approach, which the $NPZD$ model is based on, is that the ocean model data is stored directly and afterwards used for assembling the system matrices for the differential operators for the diffusion and the sinking (usually, also for the advection, which is not considered in this model) in the biogeochemical model itself. Another way is to employ the ocean model that precomputes the data to generate the necessary, so-called *transport matrices*, see [11]. These matrices usually represent a mean ocean circulation field for one month.

The time discretization is performed by a sequential integration at the discrete time steps $0 = t_0 < \ldots < t_j < \ldots < t_{n_\tau - 1} = T$ using a time step $\tau := t_j - t_{j-1}$ and with totally $n_\tau$ steps. This integration is partially implicit. An explicit euler time-stepping scheme for the nonlinear coupling terms $q_i$ and the sinking term for the tracer detritus is used while using an implicit euler time-stepping scheme for the diffusion term. Furthermore, an operator splitting method is used [18]. For details we refer the reader to [20, 22].

For the numerical simulation, one may consider a spin-up into a steady quasi-periodic or periodic seasonal cycle, thus applying some kind of fixed point iteration. Another way, which is employed in the $NPZD$ model, is to perform a complete transient run with time-dependent forcing data (as for example the temperature) to obtain a solution of (9). Assuming $n_z$ and $n_\tau$ discrete spatial and temporal grid points, with a time step $\tau = T/n_\tau$ and using a boldfaced notation for discrete vectors in the following, we denote by

$$\mathbf{y}_i = (\mathbf{y}_{ijk})_{\substack{j=1,\ldots,n_\tau \\ k=1,\ldots,n_z}} \tag{14}$$

the approximate solution of (9), i.e., $\mathbf{y}_{ijk} \approx y_i(t_j, z_k)$, denoting the concentration of tracer $i$ at the discrete time step $j$ and vertical depth layer $k$. The four state vectors for the tracers dissolved inorganic nitrogen ($N$), phytoplankton ($P$), zooplankton ($Z$) and detritus ($D$) as well as the state for the additional carbon primary production ($CUP$) will be summarized in the discrete vector $\mathbf{y} = (\mathbf{y}_i)_{i=1,\ldots,5}$ in the following.

*4.3. Original Fine Model*

In the *original* discrete model, the time step $\tau$ is chosen as one hour. By chosing this time step all relevant processes are captured and further decrease of the time step does not improve the accuracy of the model. The number of vertical depth layers $n_z$ and discrete time steps $n_\tau$ is 66 and 43800, respectively.

From now on, we will refer to this model and corresponding discrete solution as the *original* high-fidelity or fine model and will denote its state variable, time step and number of overall discrete time steps, to be distinguishable from the coarse model, by $\mathbf{y}_f$, $\tau_f$ and $n_{\tau,f}$, respectively.

*4.4. Original Fine Model Optimization Problem*

The optimization problem consists of finding *optimal* parameters yielding a minimal misfit of the discrete model response $\mathbf{y}_f$ to measurement data $\mathbf{y}_d$ as defined by the least-squares type cost function

$$\underset{\mathbf{u}\in U_{ad}}{\operatorname{argmin}}\ J_1(\mathbf{y}_f(\mathbf{u})) \tag{15}$$

where

$$\begin{aligned} J_1(\mathbf{y}_f) &:= \| C_1\,\mathbf{y}_f - \mathbf{y}_d \|_\sigma^2, \\ U_{ad} &:= \{\mathbf{u}\in\mathbb{R}^{n_p} : \mathbf{b}_l \le \mathbf{u} \le \mathbf{b}_u\}, \mathbf{b}_l, \mathbf{b}_u \in \mathbb{R}^{n_p}, \mathbf{b}_l < \mathbf{b}_u. \end{aligned} \tag{16}$$

More specifically, the measurement data $\mathbf{y}_d$ is considered for the years 1991-1995 and is taken from the *Bermuda Atlantic Time-Series Study*, called BATS, located at $31°N$, $64°W$ [27]. The inequalities in (16) in the definition of the set $U_{ad}$ of admissible parameters are meant component-wise. The parameters $\mathbf{u}$ are the unknown scalar coefficients in the nonlinear biogeochemical coupling terms $q_i$ in (9). The specific parameter bounds $\mathbf{b}_u, \mathbf{b}_l$ that we employ in the optimization runs in this paper are provided in Table 3.

Furthermore, we have $n_p = 12$ model parameters subject to optimization (cf. Table 1) and the norm is weighted by assumed standard deviations of the measurements, $\sigma = (\sigma_j)_{j=1\ldots,5}$ (see [25, 27] for details).

The functional $J_1$ may additionally include a regularization term for the parameters, which turned out to be not necessary to yield sufficient performance in the optimization runs in this paper. Additional constraints on the state variable $\mathbf{y}$ might be necessary, e.g., to ensure non-negativity of the tracer concentrations. In our example model, this is ensured by using appropriate parameter bounds $\mathbf{b}_l$ and $\mathbf{b}_u$. This was already observed and used in [25].

$C_1$ is an operator describing transformations of the model response $\mathbf{y}_f$, to make it commensurable with the given measurement data $\mathbf{y}_d$. More specifically, this operator includes the following transformation:

- A linear transformation to *chlorophyll a* (denoted as $CHL$) as a function of phytoplankton $P$, using a constant conversion factor.
- A linear transformation to *particulate organic nitrogen* (denoted as $PON$), calculated as the sum of phytoplankton $P$, zooplankton $Z$ and detritus $D$.
- A spatial average of model response if the considered measurement data point lies in between two adjacent spatial grid cells
- For zooplankton, a vertically averaged concentration in the water column down to the given depth of the measurement point (which is approximately 200 meters) is calculated.
- The observed zooplankton (with state $(\mathbf{y}_d)_3$) is furthermore transformed to $(\mathbf{y}_d)_3 = 1.23 \cdot (\mathbf{y}_d)_3 + 0.097$ in order to attempt an estimate of the total zooplankton from the measured mesozooplankton biomasss (for the sake of simplicity, this is omiited in our cost function formulation (16))
- A constant temporal alignment of the model response is employed to make it commensurable with the measurement data point in time
- A 24-hourly temporal mean of the modeled carbon primary production $CUP$ is calculated to make it commensurable with observations from 24-hourly incubation measurements.

Except for zooplankton, only the data in the so-called *euphotic zone* – equivalent to the upper 20 discrete vertical depth layers in the model – is considered. For the sake of simplicity, we

omit a more detailed description and mathematical formulation of these transformations and refer the reader to.

Consequently, the measurement data in (16) is given as $\mathbf{y}_d = (\mathbf{y}_d)_{i=1,\ldots,5}$ with $(\mathbf{y}_d)_i$ denoting the measurement state corresponding to the transformed model response $C_1\,\mathbf{y}_f$, i.e., corresponding to the concentration of dissolved inorganic nitrogen ($N$), of chlorophyll a ($CHL$), of the total zooplankton biomass ($ZOO$), of particulate organic nitrogen ($PON$) and of 24-hourly incubation measurements of the carbon primary production ($CUP$), respectively.

For this model whereas using the cost function formulation above, extensive optimization runs with different methods including local, gradient-based and also global, genetic algorithms have already been performed, see for example [25, 27]. From now on, we will refer to this optimization problem and corresponding cost function formulation as the *original* fine model one.

## 5. The Low-Fidelity Model

The way we follow here to obtain a physics-based low-fidelity (or coarse) model for the time-dependent marine ecosystem model introduced in Section 4 is to employ a coarser temporal discretization (see also Section 3.2). This has already been investigated in [22] and is just briefly recalled below.

The coarse model is based upon the same model equations (9) and (10), whereas for its numerical solution (cf. Section 4.2), a larger time step, in the following denoted as $\tau_c$, is employed with

$$\tau_c = \beta \cdot \tau_f \tag{17}$$

where we call $\beta \in \mathbb{N} \setminus \{0, 1\}$ the *coarsening factor* and where $\tau_f = 1\,\mathrm{h}$ denotes the time step employed in the original fine model solution. The spatial discretization of the coarse model is the same as for the original fine one (cf. Section 4.3). The sequential integration for the coarse model (cf. Section 4.2) is performed over $n_{\tau,c} = n_{\tau,f}/\beta$ discrete time steps, with $n_{\tau,f}$ the total number of discrete time steps employed in the original fine model solution. In the following, the state variable of the coarse model will be denoted by $\mathbf{y}_c$, respectively.

Clearly, the choice of the temporal discretization, or equivalently, the coarsening factor $\beta$, determines the quality of the coarse model and of a surrogate if based upon the latter one. Moreover, both the computational cost, the performance and quality of the solution obtained by a SBO process might be affected. Overall, we seek for a reasonable trade-off between the accuracy and speed of the coarse model. This has already been investigated in [22], where a value of $\beta = 40$ turned out too be a reasonable choice.

Furthermore, it could be demonstrated that, for the given sequential integration approach used to solve for a discrete solution of the model equations (cf. Section 4.2), a numerically stable solution [8] can be obtained if additionally restricting the parameter $u_{12}$, i.e., the sinking velocity (cf. (10)), by using an appropriate upper bound. More specifically, from visual inspection of the model responses and from various optimization experiments, it turned out that $(b_u)_{12} = 5$ (cf. Table 3) for the given coarsening factor $\beta = 40$ ensures that the resulting coarse model response does not contain any numerical instabilities, at least none, which seemed to significantly influence the optimization performance.

It is worth noticing that, when applying a slight modification of the sequential integration approach by employing an implicit Euler time-stepping scheme for the sinking term, a numerically stable solution can be ensured without restrictions to the sinking velocity, which was verified by numerical experiments. Clearly, a more thorough inspection of the latter as well as a more mathematical investigation of the conditions for the numerical stability will be useful to show the full capabilities of our approach.

Given the chosen temporal discretization with $\beta = 40$, we obtain for the discrete coarse model response $n_{\tau,c} = n_{\tau,f}/\beta = 43800/40 = 1095$ discrete time steps whereas the spatial vertical discretization with $n_z = 66$ is kept fixed.

## 6. The Surrogate

In this paper, the surrogate is obtained by a multiplicative response correction approach. It turned out that this multiplicative way of correcting the coarse model response is quite suitable for the considered problem because the overall "shape" of the coarse model response resembles that of the fine one and the relation between the coarse and the fine model responses is rather well preserved while moving from one parameter vector to another. This

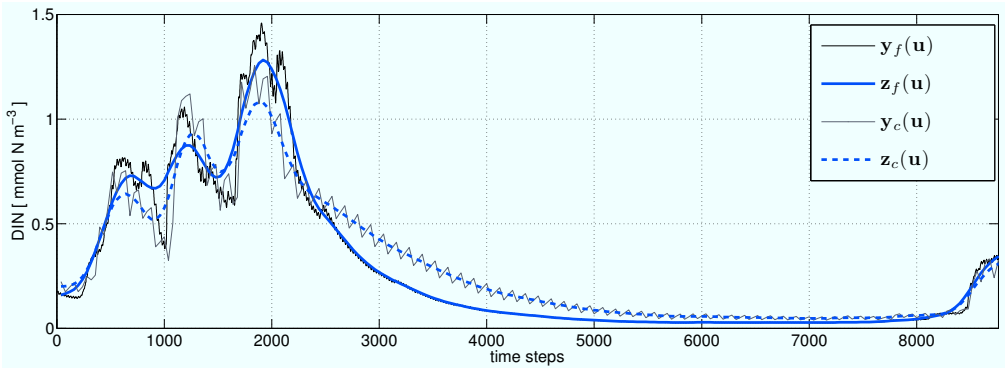


Figure 2: Fine and coarse model responses, both "raw" $(\mathbf{y}_f, \mathbf{y}_c)$ and smoothed $(\mathbf{z}_f, \mathbf{z}_c)$, employing a discrete time step of $\tau_f = 1\,\mathrm{h}$ for the fine and $\tau_c = 40\,\mathrm{h}$ for the coarse model, respectively (cf. Section 5). Shown is the response for one illustrative tracer (here, $N$), at some depth layer, part of the whole time interval and some parameter vector $\mathbf{u}$.

technique has already been investigated in [22]. We briefly recall the key ideas and describe modifications employed for the considered optimization problem below.

### *6.1. Smoothing*

Due to the larger time step employed in the numerical solution of the coarse model (cf. Section 5), the coarse model response is rather inaccurate. In [22], it has been demonstrated that "smoothing" of the coarse model response is reasonable such that the resulting smoothed response contains and tracks the main characteristics of the fine one (cf. Figure 2). Since multiplicative correction to create the surrogate is obtained by both, the coarse and the fine model response, we accordingly apply this smoothing to the fine one.

The smoothed fine and coarse model response (using an operator $S$) for the tracers $N, P, Z$ and $D$ is briefly written as

$$(\mathbf{z}_f)_i := S(\bar{\mathbf{y}}_f)_i, \quad (\mathbf{z}_c)_i := S(\mathbf{y}_c)_i, \quad i = 1, \ldots, 4 \tag{18}$$

where we consider the *down-sampled* fine model response $\bar{\mathbf{y}}_f$ given by

$$\begin{aligned} &\bar{\mathbf{y}}_f := G\mathbf{y}_f, \quad (\bar{y}_f)_{i,j,k} := (y_f)_{i,\beta j,i}, \\ &i = 1, \ldots 5, \quad j = 1, \ldots, n_{\tau,c}, \quad i = 1, \ldots, n_z \end{aligned} \tag{19}$$

to be commensurable with the corresponding coarse model response.

For the smoothing we use a *walking average* with span $\pm n$, where a value of $n = 3$ and "double" smoothing turned out to be suitable for the considered coarse model (see [22] for details). Figure 2 shows the fine and coarse model responses, both "raw" and smoothed, for the chosen temporal discretization with a coarsening factor of $\beta = 40$, for one illustrative tracer (here, $N$), some depth layer, part of the whole time interval and for some parameter vector $\mathbf{u}$.

Note that Figure 2 shows one selected tracer for some illustrative section in the whole time interval and at one selected depth layer. The total number of depth layers is 66 and the entire discrete time scale is 43800 so that it is impossible to present a full model response here. We emphasize that shown responses are representative for the overall qualitative behavior of the other tracers, time sections and depth layers which also holds for all subsequent plots shown in this paper.

*6.1.1. Treatment of the Carbon Primary Production*

The original (i.e., not down-sampled as in (19)) fine model response for the carbon primary production obeys a daily cycle (cf. Section 4.1) as shown in Figure 3a.

When employing a coarser temporal discretization using a coarsening factor of $\beta = 40$, or when down-sampling the fine model response accordingly (cf. Figure 3a), it is clearly not possible to resemble this high-frequent fine model response with a period of 24 hours. Note, that this would instead require a time step smaller than the period of the main features in the reference response, i.e., $\tau_c < 24$ (or, equivalently, $\beta < 24$).

However, as was described in Section 4.4, a 24-hourly temporal mean is applied to the original fine model response for the state $CUP$ to be commensurable with the measurement data. Hence, for the considered optimization problem, an approximation of this temporal mean would be sufficient.

Given the original, hourly fine model response for $CUP$, approximately half of the points within one interval of 24 hours are zero (cf. Figure 3a). One way to approximately obtain the temporal average would thus be to calculate a polygonal line over single positive points within each 24 hourly interval and by subsequent division by the factor two.

For the coarse model response, we accordingly apply an interpolation over all positive

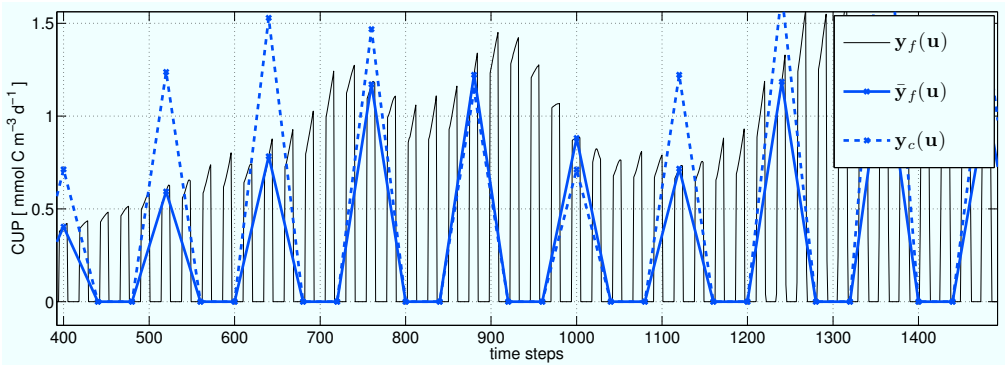


(a) Original fine, down-sampled fine and coarse model response for the state $CUP$.

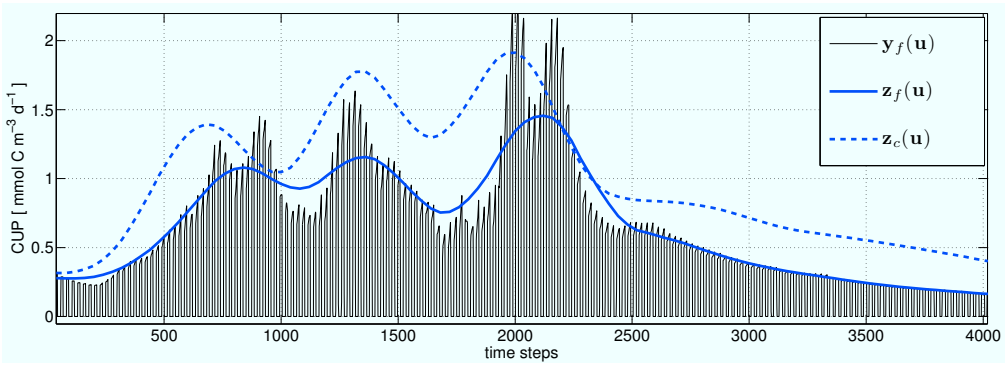


(b) Original fine, and those responses after interpolation and smoothing was applied.

Figure 3: Fine (original and down-sampled) and coarse model response, $\mathbf{y}_f$, $\bar{\mathbf{y}}_f$ and $\mathbf{y}_c$ (Figure 3a) for the carbon primary production ($CUP$), at some illustrative depth layer (here, the uppermost) and some parameter vector $\mathbf{u}$. Figure 3b shows again the original fine model response $\mathbf{y}_f$ as well as the down-sampled fine and coarse model response after interpolation and smoothing has been applied, yielding $\mathbf{z}_f$ and $\mathbf{z}_c$.

points, which provides an approximation of this envelope. More specifically, as a simple approach, we employ a piece-wise constant interpolation. Note that the subsequent division by the factor two (to obtain an approximation of the 24-hourly mean of the original fine model response) will be correspondingly included in the cost function formulation which we use for the coarse model optimization (cf. Section 7.2).

As described in Section 4.1, the carbon primary production, $CUP$, depends non-linearly on the tracers dissolved inorganic nitrogen ($N$) and phytoplankton ($P$). It is calculated internally in the model simulation and provided as an additional part of the model response.

Since the smoothing applied to the tracers $N, P, Z$ and $D$ as given in the last Section is employed outside of the model simulation, we accordingly also have to smoothen the response for $CUP$. Another approach would be to calculating CUP from the smoothed responses of $N$

and $P$ instead. Clearly, an investigation of the difference when employing the two approaches would be useful.

The smoothing is applied in the same way as for the tracers $N$, $P$, $Z$ and $D$ as described in the last Section (cf. Figure 3b).

Again, since the multiplicative correction which we use to create the surrogate is obtained by both the coarse and the (down-sampled) fine model response, the same operations, i.e., interpolation and smoothing are applied to the latter one for the state $CUP$, yielding the commensurable fine model response (cf. Figure 3b).

Altogether, we briefly write for the model state for $CUP$

$$(\mathbf{z}_f)_5 := SI(\bar{\mathbf{y}}_f)_5, \quad (\mathbf{z}_c)_5 := SI(\mathbf{y}_c)_5, \tag{20}$$

with $S$ denoting the sampling operator, $I$ the one describing the applied interpolation and where $\bar{\mathbf{y}}_f$, again, denotes the down-sampled fine model response as defined by (19).

*6.2. Surrogate Construction*

The surrogate in iteration $k$, denoted as $\mathbf{s}_k$, is obtained by a multiplicative correction of the coarse model response at the iterate $\mathbf{u}_k$. Before, the response for $CUP$ is interpolated as motivated above and smoothing to all five states is applied as described in Section 6.1.

The *correction factor*, denoted as $a_k$, is given by the point-wise division of the (down-sampled) and smoothed fine by the smoothed coarse model response (cf. 18) at the iterate $\mathbf{u}_k$, i.e.,

$$\mathbf{a}_k := \frac{\mathbf{z}_f(\mathbf{u}_k)}{\mathbf{z}_c(\mathbf{u}_k)}, \quad k = 1, 2, \ldots \tag{21}$$

where the smoothed responses $\mathbf{z}_f$ and $\mathbf{z}_c$ are given by (18) and (20) and the correction factors are summarized in the vector $\mathbf{a}_k$.

*6.2.1. Zero-order Consistent Surrogate*

A *zero-order consistent* surrogate $\bar{\mathbf{s}}_k$ (cf. (6)) can be simply obtained as

$$\bar{\mathbf{s}}_k(\mathbf{u}) := \mathbf{a}_k \, \mathbf{z}_c(\mathbf{u}) \tag{22}$$

where the multiplication in is again meant point-wise.

The surrogate defined in (22) does not satisfy the first-order consistency condition (i.e., agreement between 1st-order derivatives at the current iteration point) exactly. However, since the physics-based surrogate inherits substantial knowledge about the marine model under consideration its derivatives are expected to be at least similar to those of the fine model. The surrogate in (22) has been used in [22] and demonstrated to already yield a remarkably accurate solution at the cost of a few fine model evaluations only.

For the considered optimization problem in this paper, it turned out from numerical experiments that first order consistency is reasonable to further improve the accuracy of the surrogate and to locate the fine model optimum more precisely.

*6.2.2. Zero- and First-Order Consistent Surrogate*

To ensure exact first-order consistency with the fine model response, we furthermore include an additive correction term $E_k$ in the formulation (22) as follows

$$\begin{aligned} \mathbf{s}_k(\mathbf{u}) &:= \bar{\mathbf{s}}_k(\mathbf{u}) + E_k\,(\mathbf{u} - \mathbf{u}_k), \\ E_k &:= \mathbf{z}'_f(\mathbf{u}_k) - \bar{\mathbf{s}}'_k(\mathbf{u}_k), \end{aligned} \tag{23}$$

where $\mathbf{z}'_f$ and $\bar{\mathbf{s}}'$ denote the derivatives of the smoothed coarse and (down-sampled) fine model response, defined by (8), and where the term $\bar{\mathbf{s}}_k$ is defined by (22).

Obviously, the surrogate in (23) satisfies the zero- as well as first-order consistency condition with the fine model response in the point $\mathbf{u}_k$, more specifically with the down-sampled and smoothed response (cf. Section 6.1) as

$$\mathbf{s}_k(\mathbf{u}_k) = \mathbf{z}_f(\mathbf{u}_k), \quad \mathbf{s}'_k(\mathbf{u}_k) = \mathbf{z}'_f(\mathbf{u}_k). \tag{24}$$

*6.2.3. Improvements of the Basic Surrogate Formulation*

Occasionally, there might occur a situation where the coarse model response is close to zero (and maybe even negative due to approximation errors) and a few magnitudes smaller than the fine one, which leads to large (possibly negative) correction factors $a_k$. While such a correction ensures zero-order consistency at the point where it was established (i.e., $\mathbf{u}_k$),

it may lead to (locally) poor approximation in the vicinity of this point. Resulting "spikes" appearing in the response due to large values of the correction term can be viewed, in a way, as a numerical noise that slows down the algorithm convergence and makes the optimum more difficult to locate. This has already been investigated in [21], where an upper bound for $a_k$ as well as a non-negative bound for the coarse model response (the negative response is non-physical and is a result of large time steps employed in the coarse model solution) has been suggested to address these issues.

More specifically, we apply the following modifications at each iteration $k$ of an SBO run (cf. (5)):

$$(i)\ \mathbf{y}_c = \begin{cases} 0; & \text{if } \mathbf{y}_c \leq 0 \\ \mathbf{y}_c; & \text{else} \end{cases},\ (ii)\ \mathbf{a}_k = \begin{cases} a_{\text{ub}}; & \text{if } \mathbf{a}_k \geq a_{\text{ub}} \\ \mathbf{a}_k; & \text{else} \end{cases},$$
$$(iii)\ \mathbf{a}_k = 1 \text{ if } (\mathbf{z}_c \leq \delta \text{ and } \mathbf{z}_f \leq \delta), \tag{25}$$

where the operations are again meant point-wise, where (i) is applied before smoothing and where $\delta$ should be of the order of the discretization error below which the responses can be treated as zero. For the considered problem, $a_{\text{ub}} = 5$ turned out to be a reasonable choice and we furthermore consider $\delta = 10^{-4}$.

Clearly, as a consequence of restricting the correction factors $a_k$ as in (25), the zero-order consistency condition in (24) can only be satisfied approximately, i.e.,

$$\mathbf{s}_k(\mathbf{u}_k) = \mathbf{z}_f(\mathbf{u}_k) + \epsilon \tag{26}$$

with $\epsilon$ thus denoting the difference between the corrected coarse model and the fine model response in the point $\mathbf{u}_k$. Although consistency in the first-order derivative of the surrogate model (23) and the fine model response as in (24) is nevertheless satisfied, agreement in the first-order derivative of the corresponding cost function values is not, as is explained below.

Assuming a general Euclidean least-squares norm $J$, measuring the misfit between the

model response $\mathbf{y}$ and some specification $\mathbf{y}_d$, the gradient $J'$ is given by

$$\begin{aligned} J'(\mathbf{y}) &= \left.\frac{\mathrm{d}J(\mathbf{y})}{\mathrm{d}\mathbf{u}}\right|_{\mathbf{u}=\mathbf{u}_k} = \big(\mathbf{y}(\mathbf{u}_k) - \mathbf{y}_d\big)^T \, \mathbf{y}'(\mathbf{u}_k), \\ J(\mathbf{y}) &:= \frac{1}{2} \, \| \, \mathbf{y}(\mathbf{u}) - \mathbf{y}_d \, \|_2^2. \end{aligned} \tag{27}$$

The surrogate's cost function gradient is thus given by

$$\begin{aligned} J'(\mathbf{s}_k(\mathbf{u}_k)) &= \big(\mathbf{s}_k(\mathbf{u}_k) - \mathbf{y}_d\big)^T \, \mathbf{s}_k'(\mathbf{u}_k) \\ &= \big(\mathbf{z}_f(\mathbf{u}_k) + \epsilon - \mathbf{y}_d\big)^T \, \mathbf{z}_f'(\mathbf{u}_k). \end{aligned} \tag{28}$$

Clearly, exact agreement in the cost function gradients, i.e., $J'(\mathbf{s}_k(\mathbf{u}_k)) = J'(\mathbf{z}_f(\mathbf{u}_k))$, can only be satisfied exactly, if, besides the first-order consistency, also exact zero-order consistency as is in (24) is ensured, i.e., if $\epsilon = 0$.

It is not clear, whether an exact agreement in the first-order derivative is actually necessary in practice. Nevertheless, we use another additive term, denoted as $D_k$, in the definition of the surrogate (23), that allows us to eliminate any possible influence of the problem described above. The surrogate, which we finally employ in the optimization, is formulated as

$$\begin{aligned} \mathbf{s}_k(\mathbf{u}) &:= \bar{\mathbf{s}}_k(\mathbf{u}) + D_k + E_k \, (\mathbf{u} - \mathbf{u}_k), \\ D_k &:= \mathbf{z}_f(\mathbf{u}_k) - \bar{\mathbf{s}}_k(\mathbf{u}_k) = \epsilon, \end{aligned} \tag{29}$$

where the terms $\bar{\mathbf{s}}_k$ and $E_k$ are defined in (22) and (23) and where the underlying correction factors $a_k$ are restricted as suggested in (25).

The surrogate in (29) now satisfies exact zero- and first-order consistency, both with the fine model response $\mathbf{z}_f$ as well as with its cost function value $J(\mathbf{z}_f)$ in the current point $\mathbf{u}_k$.

## 7. Optimization Setup

The operation and performance of the proposed surrogate-based algorithm is illustrated through the results of exemplary optimization runs with $n_z = 33, n_{\tau,f} = 8760 \cdot 5$ and $\beta = 40$, which means that we obtain $n_{\tau,c} = n_{\tau,f}/\beta = 1095$ discrete time steps for the coarse model.

The specific choice of $\beta$ has been motivated in Section 5 (see also [22]). In [24] it has already been demonstrated that, at least from point of view of the optimization results, the vertical model grid can be reduced to $n_z = 33$ depth layers, instead of the originally employed 66. Optimization of both models yield practically identical results w.r.t. parameter match and quality of the solution.

We compare the quality of the solution and the computational cost of the surrogate-based optimization to what can be obtained by a direct fine and coarse model optimization. The quality of the solutions is assessed by visual inspection of the model response and inspection of the corresponding cost function and parameter values. The computational costs of the distinct optimization processes is measured in so-called *equivalent* fine model evaluations (cf. Section 7.5). For all optimization runs we used the MATLAB[2] function `fmincon`, exploiting the active-set algorithm.

As has been verified in [25], the solution obtained by using both local, gradient-based and global, genetic algorithms, provided no suitable fit of the target. Obtaining a better result with other optimization methods seems not very likely. Thus we tentatively accept the found minima in [25] and argue that the $NPZD$ model in the current formulation will have to be changed or extended to yield a better quality of the fit.

However, it should not be the focus of this paper to further address this issue. Our aim is to demonstrate the applicability of the proposed approach to the parameter optimization of the considered model. More specifically, the focus is to demonstrate that, by exemplary optimization runs, SBO is able to yield a solution close to the one obtained by a direct fine model optimization at a low optimization cost.

It is worth noticing that, given attainable measurement data on the other hand, firstly, fine model optimization is able to reconstruct the target and corresponding optimal parameters (i.e., the discrete model is well suited for parameter identification, see [25]) and, secondly, the performance of SBO would be similar, i.e., a solution close to the target can be obtained at remarkably low computational costs. In [22], this has been verified using model-generated, attainable target data, where a surrogate as formulated in (22) has been employed in an

[2]MATLAB is a registered trademark of The MathWorks, Inc., http://www.mathworks.com

illustrative SBO run.

For the fine and coarse model optimization, we furthermore employ a random search algorithm prior to the MATLAB's gradient-based `fmincon`. This turned out to be quite suitable for the considered problem to locate a rough solution initially at low computational costs (since no sensitivity data is used). More specifically, we use 500 model evaluations within this algorithm, which turned out to yield a reasonable trade-off between the accuracy of the solution and the optimization cost.

We furthermore utilize the optimal solution obtained by the coarse model optimization as initial guess for the SBO run. In numerical tests it turned out that the accuracy of the coarse model response is sufficient to obtain an approximate solution in a first step. Most importantly, this solution is obtained at a very low optimization cost since we do not use any information from the fine model within this optimization process.

### *7.1. Reference Fine Model*

To be precise, we have to distinguish between two fine model responses and corresponding optimization problems.

Firstly, we consider the optimization of the *original* fine model for comparison which has been utilized in [24] for example and which we briefly described in Section 4.4. Recalling, original denotes the fine model with a time step of $\tau_f = 1\,\mathrm{h}$ where no further operations such as down-sampling and smoothing have been applied.

However, the coarse model response, due to the employed coarser temporal discretization and applied smoothing is supposed to provide an approximation of the down-sampled and smoothed fine model response $\mathbf{z}_f$. Moreover, by definition, the surrogate, as proposed in (29), is zero- and first-order consistent with the transformed fine model response $\mathbf{z}_f$ (cf. (24)).

Consequently, in order to obtain a fair comparison, the *down-sampled* and *smoothed* fine model response and corresponding optimization has to be treated as the actual reference. A formulation of the corresponding reference cost function is provided below in Section 7.2. A well performing surrogate-based algorithm, exploiting the proposed surrogate, is thus expected converges to at least a local minimum of this *reference optimization problem* (cf. Section 3.3).

The difference in original and reference fine model solution is mainly due to the down-sampling and smoothing which we apply to the fine model but, here, as a first straightforward approach, not to the target data. It is worth noticing that given interpolated target data on the whole original fine model grid, a formulation of an equivalent optimization problem for the reference fine model (i.e., one that ensures a solution close to the original one, or, in case of nonunique solutions, one that also provides a solution of the original fine model optimization problem (15)) is rather simple since, in this case, the down-sampling and smoothing can be applied quite easily (cf. [22]). Clearly, further investigations of this issue will be neccessary to demonstrate the full capabilities of the proposed SBO approach. See also the discussion in Section 8.1.

However, even when handling the scattered measurement data as considered in the original optimization problem (i.e., no prior interpolation applied), solutions of the original and reference fine model optimization are rather close, most importantly in terms of matching the target data (cf. Section 8.1).

*7.2. Cost Function – Reference Fine, Corse and Surrogate Model Optimization*

The cost function used in conjunction with the original fine model response $\mathbf{y}_f$ has already been formulated in Section 4.4.

In this section we now propose a formulation for the reference fine (cf. Section 7.1), coarse model and for the surrogate-based optimization, which briefly reads

$$
\begin{aligned}
&J_2\,(\,\mathbf{z}\,) := \|\, C_2\,\mathbf{z} - \mathbf{y}_d\,\|_\sigma^2, \\
&\mathbf{z} = \begin{cases} \text{reference fine model response,} & \mathbf{z} = \mathbf{z}_f \\ \text{smoothed coarse model response,} & \mathbf{z} = \mathbf{z}_c \\ \text{surrogate's response at iteration } k, & \mathbf{z} = \mathbf{s}_k \end{cases}
\end{aligned}
\tag{30}
$$

where, again, we choose an Euclidean norm weighted by assumed standard deivations of the measurements $\sigma = (\sigma_j)_{j=1\ldots,5}$ and where the operator $C_2$, which has to be used to make the model response commensurable with the measurements, is similar to the one, $C_1$, used in the original cost function (cf. Section 4.4).

Differently to the operator $C_1$ in (16), the constant temporal alignment is adjusted to the

coarser temporal grid. As was motivated in Section 6.1.1, for the state $CUP$ use a simple division of the smoothed response $(\mathbf{z})_5$ by the factor two here, instead of the 24-hourly mean which is applied to original hourly fine model response for this state. Again, for the sake of simplicity, we omit any detailed formulation of the operator $C_2$.

### *7.3. Trust Region Approach*

For the SBO, we use a trust-region (TR) safeguard (cf. Section 3.3) to further increase the robustness of the optimization process, i.e., to guarantee convergence to at least a local minimum of the (reference) optimization problem. The TR radius $\delta_k$ updated as follows (cf. [4, 13]):

$$\begin{gathered}\delta_0 = 2, \quad \delta_k = \begin{cases} \delta_k / m_{\text{decr}}, & \text{if} \quad \rho_k < r_{\text{decr}} \\ \delta_k \cdot m_{\text{incr}}, & \text{if} \quad \rho_k > r_{\text{incr}} \end{cases}, \\ r_{\text{incr}} = 0.75, \quad r_{\text{decr}} = 0.01, \quad m_{\text{incr}} = 3, \quad m_{\text{decr}} = 20,\end{gathered} \tag{31}$$

with $\rho_k$ denoting the *gain ratio* in iteration $k$ defined as

$$\begin{aligned}&\rho_k := \frac{f_{\text{new}} - f_{\text{old}}}{s_{\text{new}} - s_{\text{old}}}, \\ &f_{old} := J_2(\, \mathbf{z}_f(\mathbf{u}_k)\,), \; f_{new} := J_2(\, \mathbf{z}_f(\mathbf{u}_{k+1})\,), \\ &s_{old} := J_2(\, \mathbf{s}_k(\mathbf{u}_k)\,), \; s_{new} := J_2(\, \mathbf{s}_k(\mathbf{u}_{k+1})\,).\end{aligned} \tag{32}$$

### *7.4. Stopping Criterion*

As a termination condition for the SBO, we use the absolute step size (measured in the Euclidean norm) between two successive iterates $\mathbf{u}_k$ and $\mathbf{u}_{k-1}$ as well as a lower bound for the TR radius $\delta_k$, in the following denoted by $\delta_k^{\min}$. In practive, we choose a smaller bound for TR radius than for gamma because of the large value of $m_{\text{decr}}$. The solution $\mathbf{u}_s^*$ obtained by SBO is thus defined as

$$\mathbf{u}_s^* := \left\{ \mathbf{u}_k \;\middle|\; \left(\| \mathbf{u}_k - \mathbf{u}_{k-1} \|^2 \leq \gamma\right) \;\vee\; \left(\delta_k \leq \delta_k^{\min}\right) \right\}. \tag{33}$$

An approximate solution might be sufficient as the surrogate model is not perfectly accurate anyway. Thus, in practice, it might not be necessary to run the SBO until convergence, which keeps the optimization costs low.

To trade the quality of the solution obtained by SBO against the corresponding computational costs we consider three distinct values for the threshold, more specifically

$$\{\gamma, \delta_k^{\min}\} = \{10^{-2}, 10^{-3}\}, \{10^{-4}, 10^{-5}\}, \{2.5 \cdot 10^{-5}, 2.5 \cdot 10^{-6}\}.$$

*7.5. Optimization Cost*

We measure the optimization costs of the different runs in terms of the total number of *equivalent* fine model evaluations. This means, that for the considered coarse model, $\beta$ (with $\beta = 40$ in this paper) evaluations are equivalent to (or, as expensive as) one fine model evaluation, which is a result of the chosen coarser discretization employing the factor $\beta$ (cf. Section 5). On the other hand, the cost of one iteration of the surrogate-based optimization (O.4) (in terms of equivalent fine model evaluations) equals to the number of coarse model evaluations necessary to optimize the surrogate model divided by this factor $\beta$, and increased by the cost for the response correction.

For the proposed surrogate in (29), the cost for the correction is approximately given by 13 equivalent fine model evaluations. This mainly results from the cost for the fine model evaluation, i.e., one, plus the cost to evaluate its jacobian, which is 12 for the considered problem (since 12 model parameters are considered and finite differences are used to obtain the derivatives). The further cost of the coarse model evaluation plus its jacobian, correspondingly 13 divided by the factor $\beta = 40$, is negligible here.

*7.6. Optimization Problems and Comparison of Solutions*

In the following, we account for the solutions of both an illustrative reference (cf. Section 7.1) and original fine model optimization (cf. Section 4.4), denoted as $\mathbf{u}_{f2}^*$ and $\mathbf{u}_{f1}^*$, respectively. We further consider the solution $\mathbf{u}_c^*$ of a coarse model optimization which is used as initial guess for an illustrative SBO with its solution denoted by $\mathbf{u}_s^*$ in the following.

For the sake of brevity, results of the priorily performed random search as mentioned above are omitted in the following. The underlying cost functions have been formulated

Table 2: Optimization problems considered in this paper with $\mathbf{u}$ denoting the optimization variable. $U_{ad} := \{\mathbf{u} \in \mathbb{R}^{12} : \mathbf{b}_l \leq \mathbf{u} \leq \mathbf{b}_u\}$, denotes the space of admissible parameters with component-wise upper and lower bounds $\mathbf{b}_u$ and $\mathbf{b}_l$, respectively, as more specifically given in Table 3 (cf. Section 4.4). Cost functions $J_1$ and $J_2$ are formulated in (16) and (30). Prior to (O.1) - (O.3) we further perform a random search with an initial guess $\mathbf{u}_0$. For the sake of brevity, corresponding results are omitted here.

| $\mathbf{u}_i$ | Description | Optimization Problem |
|---|---|---|
| $\mathbf{u}_0$ | Randomly chosen initial parameter vector | |
| $\mathbf{u}^*_{f1}$ | Result of an *original* fine model optimization | $\mathbf{u}^*_{f1} := \underset{\mathbf{u}\in U_{ad}}{\operatorname{argmin}}\, J_1(\,\mathbf{y}_f(\mathbf{u})\,)$ (O.1) |
| $\mathbf{u}^*_{f2}$ | Result of a *reference* fine model optimization | $\mathbf{u}^*_{f2} := \underset{\mathbf{u}\in U_{ad}}{\operatorname{argmin}}\, J_2(\,\mathbf{z}_f(\mathbf{u})\,)$ (O.2) |
| $\mathbf{u}^*_c$ | Result of a coarse model optimization | $\mathbf{u}^*_c := \underset{\mathbf{u}\in U_{ad}}{\operatorname{argmin}}\, J_2(\,\mathbf{z}_c(\mathbf{u})\,)$ (O.3) |
| $\mathbf{u}^*_s$ | Result of a SBO run using $\mathbf{u}^*_c$ as initial guess | $\mathbf{u}_{k+1} = \underset{\mathbf{u}\in U_{ad}, \parallel \mathbf{u}-\mathbf{u}_k \parallel^2 \leq \delta_k}{\operatorname{argmin}} J_2(\,\mathbf{s}_k(\mathbf{u})\,)$ (O.4) $k = 0, 1, \ldots,\ \mathbf{u}_0 := \mathbf{u}^*_c$ |

in Sections 4.4 and 7.2. The four optimization problems (omitting the random search) are denoted as (O.1) - (O.4) and are again summarized in Table 2.

To verify the performance of the propsed method, we consider the reference fine model response $\mathbf{z}_f$ (cf. Section 7.1) and corresponding cost function value $J_2(\mathbf{z}_f)$ (cf. (30)) at the respective optima $\mathbf{u}^*_{f2}, \mathbf{u}^*_c$ and $\mathbf{u}^*_s$.

In order to also account for the solution $\mathbf{u}^*_{f1}$ obatined by the original fine model optimization (cf. Section 4.4), we accordingly present the original fine model response $\mathbf{y}_f(\mathbf{u})$ and corresponding cost function value $J_1(\mathbf{y}_f)$.

## 8. Numerical Results and Outlook

In Figure 4a, the solutions of the exemplary optimization runs as described in Section 7.6 (cf. optimization problems (O.2) - (O.4) in Table 2) are presented, comparing the reference fine model response $\mathbf{z}_f$ at the respective optima. More specifically, the Figure shows the model response which is transformed (using the operator $C_2$) to be commensurable with the given measurement data $\mathbf{y}_d$, i.e., $C_2\,\mathbf{z}_f$ (cf. Section 7.2).

The solution $\mathbf{u}_3$ obtained by SBO after 3 iterations (corresponding to a stopping criterion of $\{\gamma, \delta_k^{\min}\} = \{10^{-2}, 10^{-3}\}$), as well as – by means of the tracer Chlorophyll a – also the

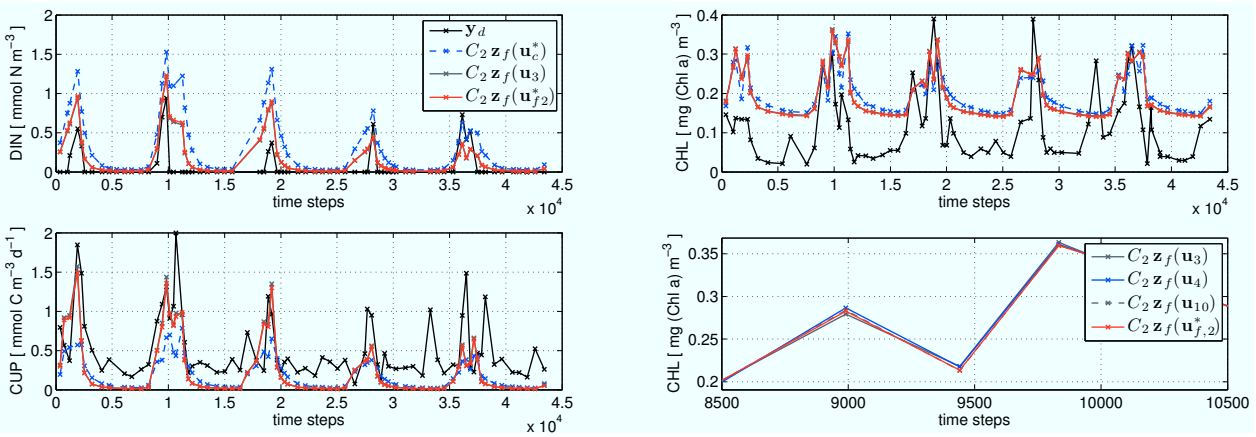


(a) Response is transformed using the operator $C_2$ to make it commensurable with the measurement data $\mathbf{y}_d$.

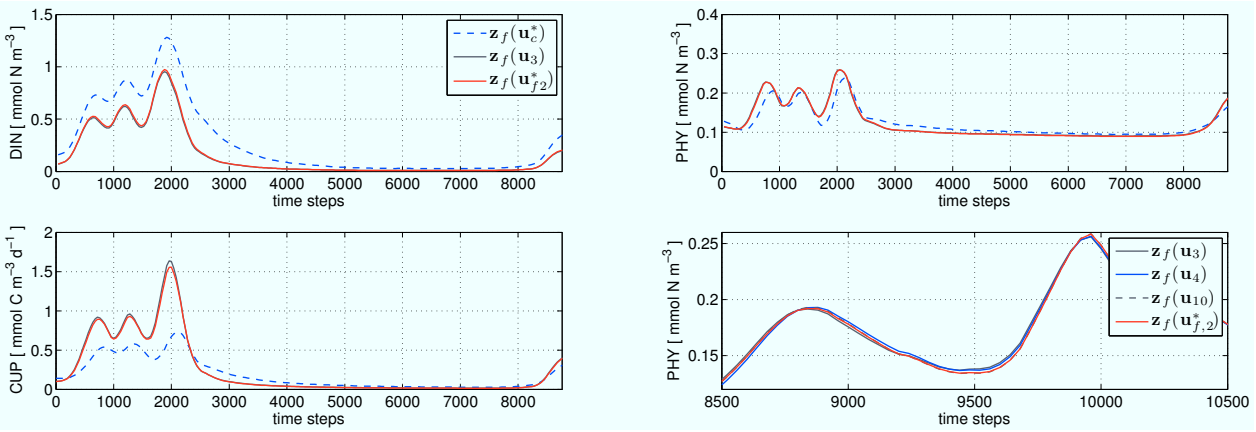


(b) Untransformed response to assess the overall quality.

Figure 4: Reference fine model response $\mathbf{z}_f$ at the solutions $\mathbf{u}_{f2}^*, \mathbf{u}_c^*, \mathbf{u}_3$ of an exemplary (reference) fine, coarse model and of a surrogate-based optimization run after three iterations (cf. Table 2). Responses are shown for three illustrative tracers, for some depth layer and in 4b, for the sake of better visibility, for a section of the whole time interval. Lower right plots: subsequent iterates $\mathbf{u}_4$ and $\mathbf{u}_{10}$ obtained in the SBO, here, by means of chlorophyll and phytoplankton and for an even smaller time section, since changes are very small.

subsequent solutions $\mathbf{u}_4$ and $\mathbf{u}_{10}$ after 4 and 10 iterations (corresponding to $\{10^{-4}, 10^{-5}\}$ and $\{2.5 \cdot 10^{-5}, 2.5 \cdot 10^{-6}\}$, respectively). In order to verify that also the overall quality of the solution obtained by SBO is sufficiently close to the one obtained by fine model optimization, we present the corresponding "untransformed" response $\mathbf{z}_f$ in Figure 4b.

It can be observed that SBO converges to the optimal solution $\mathbf{u}_{f,2}^*$ obtained by the reference fine model optimization as shown in Figures 4a, 4b, 5 and 6 (see also Table 3). Whereas coarse model optimization provides a rather inaccurate solution (i.e., far away from the reference fine one), SBO is able to yield a remarkably accuracy already after 3 iterations

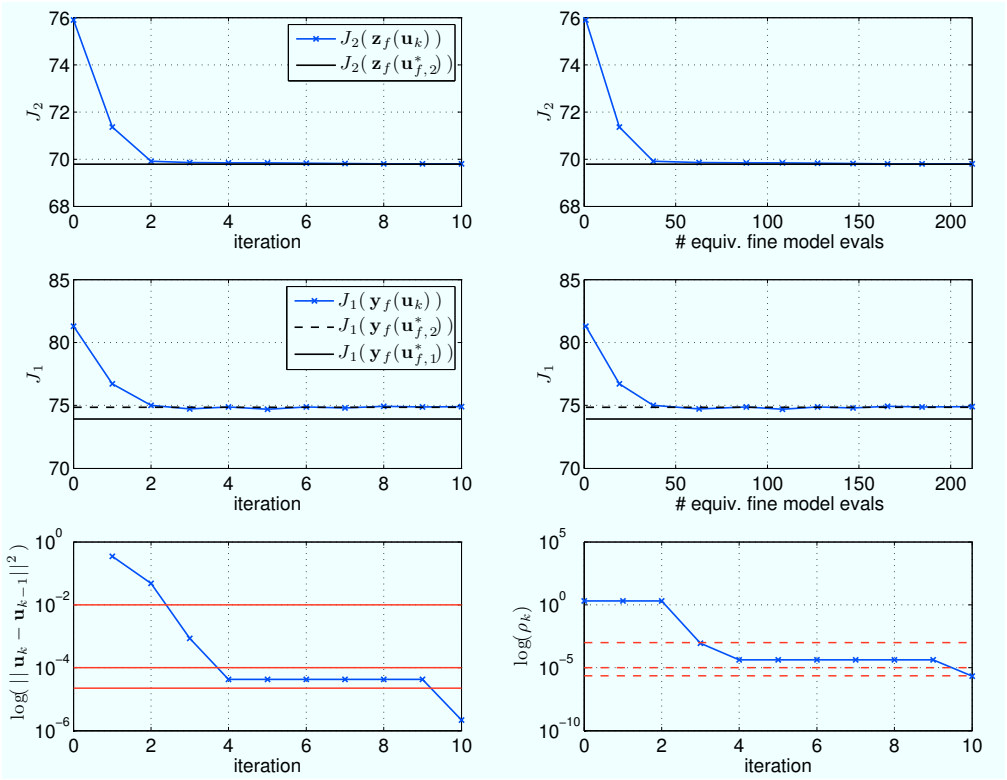


Figure 5: Optimization history of the original and the reference cost function value $J_1$ and $J_2$, both versus number of iterations and the computational costs which is measured in required *equivalent* number of fine model evaluations. Also shown are the corresponding cost function values at optimal solutions $\mathbf{u}^*_{f,1}$ and $\mathbf{u}^*_{f,2}$, obtained by the original and reference fine model optimization, the optimization history of the trust-region radius $\delta_k$ and of the squared step size norm. Horizontal red solid/dashed lines denote the distinct termination conditions considered in the SBO used to assess the solution's quality at different iterates.

– both in terms of quality of the solution (cf. Figure 4a, 4b and 5) and parameter match (cf. Figure 6 and Table 3). Only approximately 60 equivalent fine model evaluations were required (cf. Figure 5). This corresponds to a dramatical reduction in the optimization cost down to 15% of a direct fine model optimization.

Subsequently iterations within the SBO (or, equivalently, decreasing the threshold $\gamma$ used in the stopping criterion (33)), as shown in lower right plots in Figures 4a and 4b and in Figure 6 and Table 3, only slightly increases the accuracy of its solution, whereas approximately 150 additional equivalent fine model evaluations are required.

This is due to the fact that the algorithm is already very close to the fine model optimum. The accuracy of the surrogate might be not sufficient to even locate the optimal parameters

Table 3: Specific parameter values of the solutions obtained by coarse and fine (original and reference) model optimization, of iterates 3,4 and 10 obtained in a SBO run (cf. Table 2) as well as upper and lower parameter bounds $\mathbf{b}_u$ and $\mathbf{b}_l$ employed in the four optimization runs.

| iterate | $u_{k,1}$ | $u_{k,2}$ | ... | | | | | | | | | $u_{k,12}$ |
|---|---|---|---|---|---|---|---|---|---|---|---|---|
| | **Solution of SBO (O.4):** | | | | | | | | | | | |
| $\mathbf{u}_3$ | 1.000 | 1.195 | 0.052 | 0.035 | 0.024 | 4.000 | 4.000 | 0.003 | 0.089 | 0.010 | 1.000 | 5.000 |
| $\mathbf{u}_4$ | 1.000 | 1.193 | 0.052 | 0.034 | 0.026 | 4.000 | 4.000 | 0.004 | 0.095 | 0.010 | 1.000 | 5.000 |
| $\mathbf{u}_{10}$ | 1.000 | 1.176 | 0.048 | 0.035 | 0.018 | 4.000 | 4.000 | 0.004 | 0.094 | 0.010 | 1.000 | 5.000 |
| | **Solution of a coarse model optimization (O.3)** | | | | | | | | | | | |
| $\mathbf{u}_c^*$ | 1.000 | 0.522 | 0.051 | 0.040 | 0.010 | 4.000 | 4.000 | 0.007 | 0.059 | 0.010 | 0.747 | 5.000 |
| | **Solution of a (reference) fine model optimization (O.2)** | | | | | | | | | | | |
| $\mathbf{u}_{f,2}^*$ | 1.000 | 1.145 | 0.049 | 0.035 | 0.020 | 4.000 | 4.000 | 0.003 | 0.095 | 0.010 | 1.000 | 5.000 |
| | **Solution of a (original) fine model optimization (O.1)** | | | | | | | | | | | |
| $\mathbf{u}_{f,1}^*$ | 1.000 | 1.063 | 0.112 | 0.043 | 0.082 | 4.000 | 4.000 | 0.004 | 0.081 | 0.010 | 1.000 | 5.000 |
| $\mathbf{b}_l$ | 0.300 | 0.200 | 0.001 | 0.000 | 0.010 | 0.025 | 0.040 | 0.000 | 0.010 | 0.010 | 0.100 | 2.000 |
| $\mathbf{b}_u$ | 1.000 | 1.460 | 0.253 | 0.630 | 0.730 | 4.000 | 4.000 | 0.630 | 1.000 | 0.150 | 1.000 | 5.000 |

more precisely. On the other hand, the considered model is less sensitive w.r.t. some parameters which makes them more difficult to locate. This was already demonstrated in [25]. However, as was shown, the solution after 3 iterations is definitely sufficiently accurate in terms of matching the corresponding fine model response.

Furthermore, the trade-offs between the solution accuracy and the extra computational overhead related to sensitivity calculation have been investigated by additional numerical experiments. It turned out that without using fine/coarse model sensitivity, the solution of SBO is not sufficiently accurate for the considered problem, whereas, clearly, the cost savings are higher. However, using sensitivity here seems reasonable and the obtained speedup in the optimization is nevertheless remarkably high.

### *8.1. Quality of Reference and Original Fine Model Solution*

In order to also assess the difference between the solutions obtained by the reference and original fine model optimization, Figures 7a and 7b furthermore present the original fine model response at the two fine model solutions, $\mathbf{u}_{f,1}$ and $\mathbf{u}_{f,2}$.

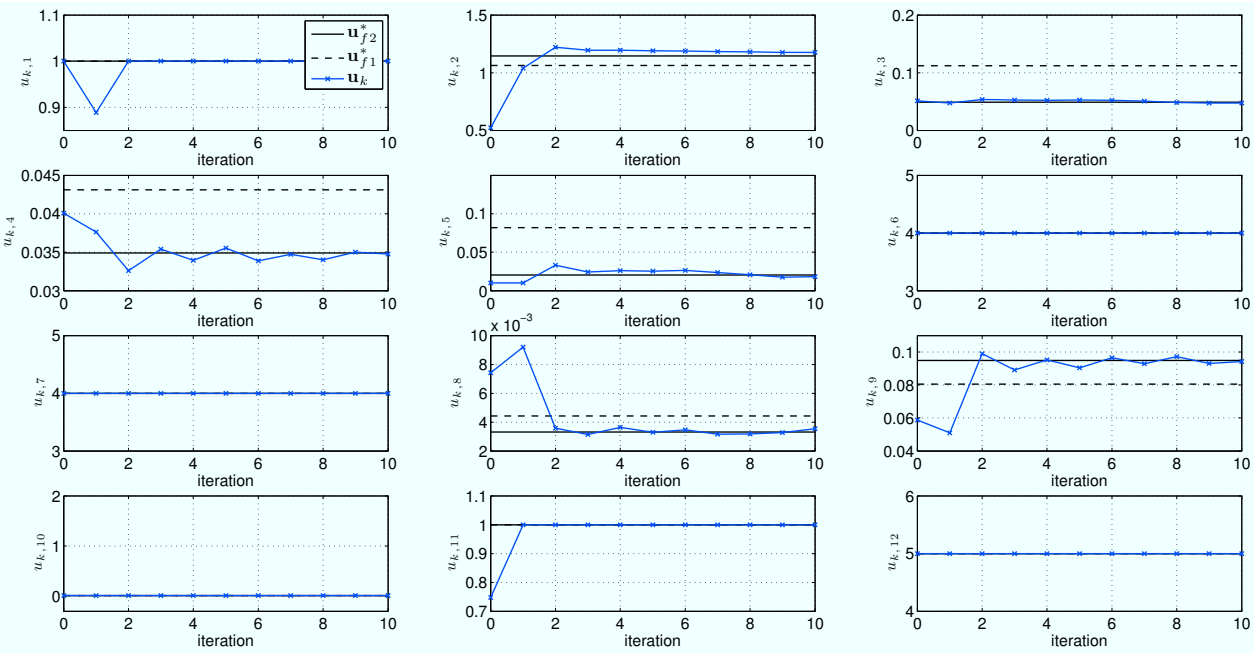


Figure 6: Optimization history of the parameters $\mathbf{u}_k$ obtained in the SBO as well as optimal parameter $\mathbf{u}^*_{f,1}$ and $\mathbf{u}^*_{f,2}$ obtained by direct fine model optimization (original and reference).

Shown is, again, the transformed (using the operator $C_1$) model response $C_2\,\mathbf{y}_f$ in Figure 7a to assess the quality and difference of the responses with respect to the given measurement data as well as the "untransformed" one, $\mathbf{y}_f$, in Figure 7b to investigate furthermore the overall quality.

Figures 5 and 6 shows the optimal parameters $\mathbf{u}^*_{f,1}$ and corresponding cost function value $J_1(\mathbf{y}_f(\mathbf{u}^*_{f,1}))$, for comparison with the corresponding values for the reference solution, $\mathbf{u}^*_{f,2}$, respectively.

It can be observed that both solutions are rather close in terms of the quality of the responses w.r.t the given measurement data and parameter match. The difference in the optimal cost function values is rather small (cf. center left plot in Figure 5). Clearly, in some time sections in the model response and for some parameters and tracers, the difference is more noticeable.

The key question to address this issue is how to formulate the reference cost function (cf. (30)), in order to yield an equivalent optimization problem. In terms of a more mathe-

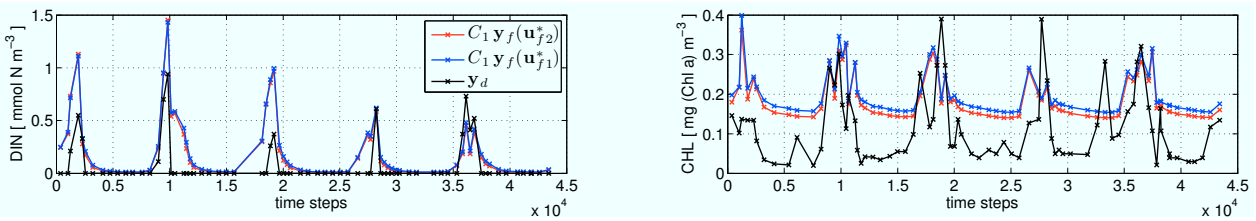


(a) Response is transformed using the operator $C_1$ to make it commensurable with the measurement data $\mathbf{y}_d$.

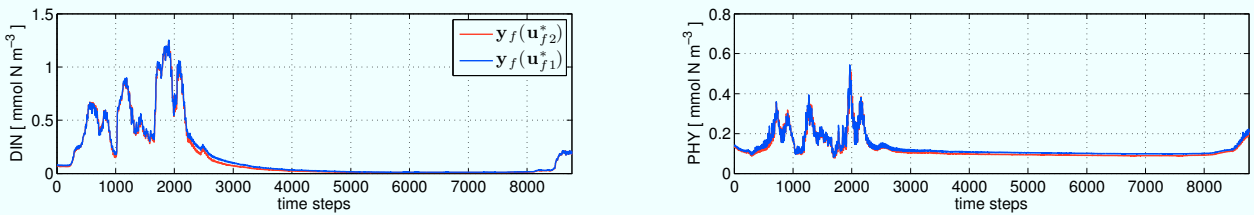


(b) Untransformed response to assess the overall quality.

Figure 7: Original fine model response $\mathbf{y}_f$, for comparison, at the solutions $\mathbf{u}^*_{f,1}$, $\mathbf{u}^*_{f,2}$ of an original and reference fine model optimization. Responses are shown for two illustrative tracers, some depth layer and in 7b, for the sake of better visibility, for a section of the whole time interval.

matical formulation, the question is how to chose and what conditions an operator $A$ in

$$J_2(\,\mathbf{z}_f\,) := \|\,C_2\,\mathbf{z}_f - A\,\mathbf{y}_d\,\|^2_\sigma \tag{34}$$

would have to satisfy. The solution is very straightforward, given interpolated target data $\mathbf{w}_d$ on the whole original fine model grid. If we assume, for the sake of simplicity, a simplified original cost function formulation

$$J_1(\,\mathbf{y}_f\,) := \|\,\mathbf{y}_f - \mathbf{w}_d\,\|^2_\sigma. \tag{35}$$

(i.e., here, the model response directly corresponds to the target data), then, the equivalent formulation for the reference cost function considering the down-sampled and smoothed fine model response $\mathbf{z}_f := SG\mathbf{y}_f$ would simply be given as

$$J_2(\,\mathbf{z}_f\,) := \|\,SG\mathbf{y}_f - SG\mathbf{w}_d\,\|^2_\sigma, \tag{36}$$

where $S$ and $G$ denote the operators for the sampling and smoothing, respectively. It is trivial that the two formulation are equivalent. As additional evidence, numerical experiments

verified that the two optimization problems (34) and (35) practically yield identical results [22].

Firstly, it is not clear, whether interpolations of the measurement data is actually reasonable. However, whether interpolations of the target are applied or not, investigations regarding these issues clearly will be necessary to show the full capabilities of this SBO approach.

## 9. Conclusions

Solving nonlinear optimization problems where computation of the objective function involves time consuming computer simulations may be quite challenging. Since typically, a large number of objective function evaluations are required, the computational costs is prohibitively high. For such problems, where the optimization of complex marine ecosystem models is a representative example, the development of methods that would reduce the number of expensive simulations necessary to yield a satisfactory solution becomes critical.

Computationally efficient optimization of expensive simulation models can be realized using surrogate-based optimization (SBO). The principal idea of SBO is to replace the high-fidelity (or fine) model in the optimization loop by its computationally cheap, but yet reasonably accurate surrogate which is updated at each iteration using available data from the fine model. For a well performing SBO, iterative updating and subsequent optimization of the surrogate can yield a remarkably accurate solution while dramatically reducing the optimization cost.

In this paper, we analyze the applicability of a surrogate obtained from a temporarily coarser discretized physics-based low-fidelity (or coarse) model. We employ a multiplicative correction to the coarse model response to obtain a reliable approximation of the fine model. As a case study, we consider a selected representative of the class of one-dimensional marine ecosystem models. This complexity of the involved processes in this model is very high. Thus, although one-dimensional, this model serves as a suitable test case before investigating computationally more expensive three-dimensional models.

A basic formulation of this approach has already been investigated in [22] and demonstrate to yield a reasonably accurate solution at low computational costs. This was verified by using

model-generated synthetic measurement data.

In this paper, we investigated the application to real data. We furthermore included enhancements of the basic formulation by utilizing coarse/fine model sensitivity data as well as trust-region convergence safeguards to further increase the robustness of the optimization process and accuracy of the solution.

We could demonstrate convergence of the SBO to the solution obtained by a direct fine model optimization. We furthermore showed that already after 3 iterations of the SBO, a solution very close to the optimal fine model one could be obtained.

Although rather expensive fine model sensitivity data was used in the SBO, optimization costs are nevertheless remarkably low – only 60 fine model, or, equivalently, 5 fine model gradient evaluations were required corresponding to a speedup of 85% when compared to the direct fine model optimization.

## 10. Acknowledgments

The authors would like to thank Andreas Oschlies, IFM Geomar, Kiel and Johannes Rückelt, Institute of Computer Science, Christian-Albrechts Universität zu Kiel. This research was supported by the DFG Cluster of Excellence Future Ocean.

## References

[1] J.W. Bandler, Q.S. Cheng, S.A. Dakroury, A.S. Mohamed, M.H. Bakr, K. Madsen, and J. Søndergaard. Space mapping: The state of the art. *IEEE T. Microw. Theory.*, 52(1), 2004.

[2] H.T. Banks and K. Kunisch. *Estimation Techniques for Distributed Parameter Systems.* Birkhäuser, 1989.

[3] H.M. Bücker, O. Fortmeier, and M. Petera. Solving a parameter estimation problem in a three-dimensional conical tube on a parallel and distributed software infrastructure. *Journal of Computational Science*, 2(2):95–104, 5 2011.

[4] A.R. Conn, N.I.M. Gould, and P.L. Toint. *Trust-region methods.* Society for Industrial and Applied Mathematics, Philadelphia, PA, 2000.

[5] D. Echeverria and P. Hemker. Manifold mapping: a two-level optimization technique. *Computing and Visualization in Science*, 11:193–206, 2008. 10.1007/s00791-008-0096-y.

[6] G.T. Evans and J.S. Parslow. A model of annual plankton cycles. *Biological Oceanography*, 3:328–347, 1985.

[7] W. Fennel and T. Neumann. *Introduction to the Modelling of Marine Ecosystems*. Elsevier, 2004.

[8] C.A.J. Fletcher. *Computational Techniques for Fluid Dynamics*, volume 1. Springer, 2nd edition, 1991.

[9] A.I.J. Forrester and A.J. Keane. Recent advances in surrogate-based optimization. *Prog. Aerosp. Sci.*, 45(1-3):50–79, 2009.

[10] A.E. Gill. *Atmosphere - Ocean Dynamics*, volume 30 of *International Geophysics Series*. Academic Press, 1982.

[11] S. Khatiwala, M. Visbeck, and M.A. Cane. Accelerated simulation of passive tracers in ocean circulation models. *Ocean Modelling*, 9(1):51–69, 2005.

[12] S. Koziel. Shape-preserving response prediction for microwave design optimization. *Microwave Theory and Techniques, IEEE Transactions on*, 58(11):2829 –2837, nov. 2010.

[13] S. Koziel, J.W. Bandler, and Q.S. Cheng. Robust trust-region space-mapping algorithms for microwave design optimization. *IEEE T. Microw. Theory.*, 58(8):2166–2174, August 2010.

[14] P. Kunkel and V. Mehrmann. *Differential-algebraic equations: analysis and numerical solution*. EMS, 2006.

[15] L. Leifsson and S. Koziel. Multi-fidelity design optimization of transonic airfoils using physics-based surrogate modeling and shape-preserving response prediction. *Journal of Computational Science*, 1(2):98–106, 6 2010.

[16] J. Liebig, L.P. Playfair, and J.W. Webster. *Chemistry in its application to agriculture and physiology*. J. Owen, 1842.

[17] A. Majda. *Introduction to PDE's and Waves for the Atmosphere and Ocean*. AMS, 2003.

[18] G.I. Marchuk. *Methods of Numerical Mathematics*. Springer, 2nd edition, 1982.

[19] K. McGuffie and A. Henderson-Sellers. *A Climate Modelling Primer*. Wiley, 3nd edition, 2005.

[20] A. Oschlies and V. Garcon. An eddy-permitting coupled physical-biological model of the north atlantic. 1. sensitivity to advection numerics and mixed layer physics. *Global Biogeochem. Cy.*, 13:135–160, 1999.

[21] M. Prieß, S. Koziel, and T. Slawig. Improved surrogate-based optimization of climate model parameters using response correction. pages 449–457, Noordwijkerhout, The Netherlands, July 2011. Int. Conf. Simulation and Modeling Methodologies, Technologies and Appl., SIMULTECH 2011.

[22] M. Prieß, S. Koziel, and T. Slawig. Surrogate-based optimization of climate model parameters using response correction. *Journal of Computational Science*, (0):1877–7503, 2011.

[23] N.V. Queipo, R.T. Haftka, W. Shyy, T. Goel, R. Vaidyanathan, and P.K. Tucker. Surrogate-based analysis and optimization. *Prog. Aerosp. Sci.*, 41(1):1–28, 2005.

[24] J. Rückelt, A. Oschlies, and T. Slawig. Optimization of parameters and initial values in a marine NPZD-type ecosystem model. Technical Report 1013, CAU Kiel, Institut für Informatik, 2010.

[25] J. Rückelt, V. Sauerland, T. Slawig, A. Srivastav, B. Ward, and C. Patvardhan. Parameter optimization and uncertainty analysis in a model of oceanic $CO\_2$-uptake using a hybrid algorithm and algorithmic differentiation. *Nonlinear Analysis B Real World Applications*, 10(1016):3993–4009, 2010.

[26] J.L. Sarmiento and N. Gruber. *Ocean Biogeochemical Dynamics*. Princeton University Press, 2006.

[27] M. Schartau and A. Oschlies. Simultaneous data-based optimization of a 1d-ecosystem model at three locations in the north atlantic: Part i - method and parameter estimates. *Journal of Marine Research*, 61:765–793, 2003.

[28] T.W. Simpson, J.D. Poplinski, P.N. Koch, and J.K. Allen. Metamodels for computer-based engineering design: Survey and recommendations. *Eng. Comput.*, 17:129–150, 2001. 10.1007/PL00007198.

[29] A.J. Smola and B. Schölkopf. A tutorial on support vector regression. *Stat. Comput.*, 14:199–222, 2004. 10.1023/B:STCO.0000035301.49549.88.

[30] J. Søndergaard. *Optimization using surrogate models - by the space mapping technique.* PhD thesis, Informatics and Mathematical Modelling, Technical University of Denmark, DTU, Richard Petersens Plads, Building 321, DK-2800 Kgs. Lyngby, 2003. Supervisor: Kaj Madsen.

[31] A. Tarantola. *Inverse Problem Theory and Methods for Model Parameter Estimation.* SIAM, 2005.